Structural Engineering and Mechanics, *Vol. 55, No. 5 (2015) 1001-1014*
DOI: http://dx.doi.org/10.12989/sem.2015.55.5.1001

Size-dependent bending analysis of FGM nano-sinusoidal plates resting on orthotropic elastic medium

Reza Kolahchi*[1], Ali Mohammad Moniri Bidgoli[2] and Mohammad Mehdi Heydari[3]

[1]Department of Mechanical Engineering, Shahinshahr Branch, Islamic Azad University, Shahinshahr, Iran
[2]Faculty of Mechanical Engineering, College of Engineering, University of Tehran, Tehran, Iran
[3]Young Researchers and Elite Club, Kashan Branch, Islamic Azad University, Kashan, Iran

(Received March 11, 2015, Revised July 26, 2015, Accepted July 31, 2015)

Abstract. Bending analysis of functionally graded (FG) nano-plates is investigated in the present work based on a new sinusoidal shear deformation theory. The theory accounts for sinusoidal distribution of transverse shear stress, and satisfies the free transverse shear stress conditions on the top and bottom surfaces of the plate without using shear correction factor. The material properties of nano-plate are assumed to vary according to power law distribution of the volume fraction of the constituents. The size effects are considered based on Eringen's nonlocal theory. Governing equations are derived using energy method and Hamilton's principle. The closed-form solutions of simply supported nano-plates are obtained and the results are compared with those of first-order shear deformation theory and higher-order shear deformation theory. The effects of different parameters such as nano-plate length and thickness, elastic foundation, orientation of foundation orthtotropy direction and nonlocal parameters are shown in dimensionless displacement of system. It can be found that with increasing nonlocal parameter, the dimensionless displacement of nano-plate increases.

Keywords: FG nano-plate; sinusoidal shear deformation theory; exact solution; bending

1. Introduction

Functionally graded materials (FGMs) are a class of composites that have continuous variation of material properties from one surface to another and thus eliminate the stress concentration found in laminated composites. FGMs are widely used in many structural applications such as mechanics, civil engineering, aerospace, nuclear, and automotive. In company with the increase in the application of FGM in engineering structures, many computational models have been developed for predicting the response of FG plates. These models can either be developed using displacement-based theories (when the principle of virtual work is used) or displacement-stress-based theories (when Reissner's mixed variational theorem is used). In general, these theories can be classified into three main categories: classical plate theory (CPT); first-order shear deformation theory (FSDT); and higher-order shear deformation theory (HSDT). The CPT, which neglects the transverse shear deformation effects, provides accurate results for thin plates (Javaheri and Eslami

*Corresponding author, Ph.D., E-mail: r.kolahchi@gmail.com

http://www.techno-press.org/?journal=sem&subpage=8 ISSN: 1225-4568 (Print), 1598-6217 (Online)

2002). For moderately thick plates, it underestimates deflections and overestimates buckling loads and natural frequencies. The FSDT accounts for the transverse shear deformation effect, but require a shear correction factor to satisfy the free transverse shear stress conditions on the top and bottom surfaces of the plate (Della Croce and Venini 2004). Although the FSDT provides a sufficiently accurate description of response for thin to moderately thick plates, it is not convenient to use due to difficulty in determination of correct value of the shear correction factor. To avoid the use of shear correction factor, many HSDTs were developed based on the assumption of quadratic, cubic or higher-order variations of in-plane displacements through the plate thickness, notable among them are Reddy (2000), Karama *et al*. (2003), Zenkour (2005), Xiao *et al*. (2007), Matsunaga (2008), Pradyumna and Bandyopadhyay (2008), Fares *et al*. (2009), Talha and Singh (2010), Benyoucef *et al*. (2010), Xiang *et al*. (2011). Among the aforementioned HSDTs, the well-known HSDTs with five unknowns include: the Reddy's theory, the sinusoidal shear deformation theory, the hyperbolic shear deformation theory, the exponential shear deformation theory. Although the HSDTs with five unknowns are sufficiently accurate to predict response of thin to thick plate, their equations of motion are much more complicated than those of FSDT and CPT. Therefore, there is a scope to develop a HSDT which is simple to use.

This paper aims to develop a simple sinusoidal shear deformation theory for bending analyses of FG nano-plates. This theory is based on assumption that the in-plane and transverse displacements consist of bending and shear parts. Unlike the conventional sinusoidal shear deformation theory, the proposed sinusoidal shear deformation theory contains four unknowns and has strong similarities with CPT in many aspects such as equations of motion, boundary conditions, and stress resultant expressions. Material properties of FG nano-plate are assumed to vary according to power law distribution of the volume fraction of the constituents. Equations of motion are derived from the Hamilton's principle including the nonlocal parameter. The closed-form solutions are obtained for simply supported nano-plates. The effects of different parameters such as nano-plate length and thickness, elastic foundation, orientation of foundation orthtotropy direction and nonlocal parameters are shown in dimensionless displacement of system.

2. Theoretical formulations

2.1 Basic assumptions

The assumptions of the present theory are as follows:

i. The displacements are small in comparison with the nano-plate thickness and, therefore, strains involved are infinitesimal.

ii. The transverse normal stress σ_z is negligible in comparison whit in-plane stresses σ_x and σ_y.

iii. The transverse displacement u_3 includes two components of bending w_b and shear w_s. These components are functions of coordinates x, y, and time t only.

$$u_3(x,y,z,t) = w_b(x,y,t) + w_s(x,y,t) \tag{1}$$

iv. The in-plane displacements u_1 and u_2 consist of extension, bending, and shear components.

$$u_1 = u + u_b + u_s \ and \ u_2 = v + v_b + v_s \tag{2}$$

- The bending components u_b and v_b are assumed to be similar to the displacements given by the classical nano-plate theory. Therefore, the expressions for u_b and v_b are

$$u_b = -z\frac{\partial w_b}{\partial x} \, and \, v_b = -z\frac{\partial w_b}{\partial y} \tag{3a}$$

The shear components u_s and v_s give rise, in conjunction with w_s, to the sinusoidal variations of shear strains γ_{xz}, γ_{yz} and hence to shear stresses σ_{xz}, σ_{yz} through the thickness h of the nano-plate in such a way that shear stresses σ_{xz}, σ_{yz} are zero at the top and bottom surfaces of the nano-plate. Consequently, the expression for u_s and v_s can be given as

$$u_s = -\left(z - \frac{h}{\pi}\sin\frac{\pi z}{h}\right)\frac{\partial w_b}{\partial y} \, and \, v_s = -\left(z - \frac{h}{\pi}\sin\frac{\pi z}{h}\right)\frac{\partial w_s}{\partial y} \tag{3b}$$

2.2 Kinematics

Based on the assumptions made in the preceding section, the displacement field can be obtained using Eqs. (1)-(3)

$$\begin{aligned} u_1(x,y,z,t) &= u(x,y,t) - z\frac{\partial w_b}{\partial x} - f\frac{\partial w_s}{\partial x} \\ u_2(x,y,z,t) &= v(x,y,t) - z\frac{\partial w_b}{\partial y} - f\frac{\partial w_s}{\partial y} \\ u_3(x,y,z,t) &= w_b(x,y,t) + w_s(x,y,t) \end{aligned} \tag{4}$$

where

$$f = z - \frac{h}{\pi}\sin\frac{\pi z}{h} \tag{5}$$

The kinematic relations can be obtained as follows

$$\begin{Bmatrix} \varepsilon_x \\ \varepsilon_y \\ \gamma_{xy} \end{Bmatrix} = \begin{Bmatrix} \varepsilon_x^0 \\ \varepsilon_y^0 \\ \gamma_{xy}^0 \end{Bmatrix} + z\begin{Bmatrix} k_x^b \\ k_y^b \\ k_{xy}^b \end{Bmatrix} + f\begin{Bmatrix} k_x^s \\ k_y^s \\ k_{xy}^s \end{Bmatrix}, \begin{Bmatrix} \gamma_{yz} \\ \gamma_{xz} \end{Bmatrix} = g\begin{Bmatrix} \gamma_{yz}^s \\ \gamma_{xz}^s \end{Bmatrix} \tag{6a}$$

where

$$\begin{Bmatrix} \varepsilon_x^0 \\ \varepsilon_y^0 \\ \gamma_{xy}^0 \end{Bmatrix} = \begin{Bmatrix} \dfrac{\partial u}{\partial x} \\ \dfrac{\partial v}{\partial y} \\ \dfrac{\partial u}{\partial y} + \dfrac{\partial v}{\partial x} \end{Bmatrix}, \begin{Bmatrix} k_x^b \\ k_y^b \\ k_{xy}^b \end{Bmatrix} = \begin{Bmatrix} -\dfrac{\partial^2 w_b}{\partial x^2} \\ -\dfrac{\partial^2 w_b}{\partial y^2} \\ -2\dfrac{\partial^2 w_b}{\partial x \partial y} \end{Bmatrix}, \begin{Bmatrix} k_x^s \\ k_y^s \\ k_{xy}^s \end{Bmatrix} = \begin{Bmatrix} -\dfrac{\partial^2 w_s}{\partial x^2} \\ -\dfrac{\partial^2 w_s}{\partial y^2} \\ -2\dfrac{\partial^2 w_s}{\partial x \partial y} \end{Bmatrix}$$
$$, \begin{Bmatrix} \gamma_{yz}^s \\ \gamma_{xz}^s \end{Bmatrix} = \begin{Bmatrix} \dfrac{\partial w_s}{\partial y} \\ \dfrac{\partial w_s}{\partial x} \end{Bmatrix}, g = 1 - \frac{df}{dz} = \cos\left(\frac{\pi z}{h}\right). \tag{6b}$$

2.3 Constitutive equations

In the Eringen's nonlocal elasticity model, the stress state at a reference point in the body is regarded to be dependent not only on the strain state at this point but also on the strain states at all of the points throughout the body. The constitutive equation for stresses $\boldsymbol{\sigma}$ and strains $\boldsymbol{\varepsilon}$ matrixes may be written as follows (Eringen 1972)

$$(1-(e_0a)^2\,\nabla^2)\sigma_{ij}=C_{ijkl}\;\varepsilon_{kl}, \tag{7}$$

where C_{ijkl} is elastic constants; e_0a denotes the small scale parameter, and ∇^2 is the Laplace operator. The material properties of FG nano-plate are assumed to vary continuously through the thickness of the nano-plate in accordance with a power law distribution as (Ameur *et al*. 1972)

$$p(z)=p_m+(p_c-p_m)(\tfrac{1}{2}+\tfrac{z}{h})^p \tag{8}$$

where p represents the effective material property such as Young's modulus E and mass density ρ. Subscripts m and c represent the metallic and ceramic constituents, respectively; and p is the volume fraction exponent. The value of p equal to zero represents a fully ceramic nano-plate, whereas infinite p indicates a fully metallic nano-plate. Since the effects of the variation of poisson'ratio on the response of FG nano-plates are very small, the Poisson's ratio (v) is usually assumed to be constant. However, the constitutive equation of nano-plate may be expressed as

$$(1-(e_0a)^2\nabla^2)\begin{Bmatrix}\sigma_x\\ \sigma_y\\ \sigma_{xy}\\ \sigma_{yz}\\ \sigma_{xz}\end{Bmatrix}=\frac{E(z)}{1-v^2}\begin{bmatrix}1 & v & 0 & 0 & 0\\ v & 1 & 0 & 0 & 0\\ 0 & 0 & \frac{(1-v)}{2} & 0 & 0\\ 0 & 0 & 0 & \frac{(1-v)}{2} & 0\\ 0 & 0 & 0 & 0 & \frac{(1-v)}{2}\end{bmatrix}\begin{Bmatrix}\varepsilon_x\\ \varepsilon_y\\ \gamma_{xy}\\ \gamma_{yz}\\ \gamma_{xz}\end{Bmatrix}. \tag{9}$$

2.4 Equations of motion

Hamilton's principle is used herein to derive the equations of motion. The principle can be stated in analytical form as

$$0=\int_0^t(\delta U+\delta V+\delta W-\delta K)dt \tag{10}$$

where δU is the variation of strain energy; δV and δW are the variation of external and in-plane loads, respectively ; and δK is the variation of kinetic energy.

The variation of strain energy of the nano-plate is calculated by

$$\partial U=\int_V\,(\sigma_x\partial\varepsilon_x+\sigma_y\partial\varepsilon_y+\sigma_{xy}\partial\gamma_{xy}+\sigma_{yz}\partial\gamma_{yz}+\sigma_{xz}\partial\gamma_{xz})dAdz=\int_A\,\Big\{N_x\frac{\partial\delta u}{\partial x}-M_x^b\frac{\partial^2\delta w_b}{\partial x^2}-M_x^s\frac{\partial^2\delta w_s}{\partial x^2}+N_y\frac{\partial\delta u}{\partial y}-M_y^b\frac{\partial^2\delta w_b}{\partial y^2}-M_y^s\frac{\partial^2\delta w_s}{\partial y^2}+N_{xy}\left(\frac{\partial\delta u}{\partial y}+\frac{\partial\delta u}{\partial x}\right)-2M_{xy}^b\frac{\partial^2\delta w_b}{\partial x\partial y}-2M_{xy}^s\frac{\partial^2\delta w_s}{\partial x\partial y}+Q_{yz}\frac{\partial\delta w_s}{\partial y}+Q_{xz}\frac{\partial\delta w_s}{\partial x}\Big\}dA \tag{11}$$

where N, M, and Q are the stress resultants defined as

$$\left(N_I,M_i^b,M_i^s\right)=\int_{-\frac{h}{2}}^{\frac{h}{2}}(1,z,f)\sigma_i dz,\;\;(i=x,y,xy) and\; Q_i=\int_{-\frac{h}{2}}^{\frac{h}{2}}g\sigma_i dz\,,i(xy,yz). \tag{12}$$

The variation of potential energy of the applied loads can be expressed as

$$\delta V=-\int_A\,(F_{elastic}+q)\delta u_3 dA \tag{13a}$$

where q is transverse loads applied on the top surface of nano-plate and $F_{elastic}$ is due to orthotropic elastic foundation which can be written as

$$F_{elastic} = kw - G_\xi\left(\cos^2\theta w_{,xx} + 2\cos\theta\sin\theta w_{,yx} + \sin^2\theta w_{,yy}\right) - G_\eta\left(\sin^2\theta w_{,xx} - 2\sin\theta\cos\theta w_{,yx} + \cos^2\theta w_{,yy}\right), \tag{13b}$$

where angle θ describes the local ξ direction of orthotropic foundation with respect to the global x-axis of the nano-plate; k, G_ξ and G_η are Winkler foundation parameter, shear foundation parameters in ξ and η directions, respectively. Furthermore, the variation of work done by the in-plane loads may be written as

$$\delta W = -\frac{1}{2}\int_A \left(N_x^0 \frac{\partial u_3}{\partial x}\frac{\partial \delta u_3}{\partial x} + N_y^0 \frac{\partial u_3}{\partial y}\frac{\partial \delta u_3}{\partial y}\right) dA, \tag{13c}$$

where N_x^0 and N_x^0 are in-plane loads in x and y directions, respectively. The variation of kinetic energy of the nano-plate can be written as

$$\partial K = \int_V (\dot{u}_1\delta\dot{u}_1 + \dot{u}_2\delta\dot{u}_2 + \dot{u}_3\delta\dot{u}_3)\,\rho(z)dAdz = \int_A \Big\{ I_O[\dot{u}\partial\dot{u} + \dot{v}\partial\dot{v} + (\dot{w}_b + \dot{w}_s)\partial(\dot{w}_b + \dot{w}_s)] - I_1\left(\dot{u}\frac{\partial\delta\dot{w}_b}{\partial x} + \dot{u}\delta\frac{\partial\dot{w}_b}{\partial x} + \dot{v}\frac{\partial\delta\dot{w}_b}{\partial y} + \delta\dot{v}\frac{\partial\dot{w}_b}{\partial y}\right) - J_1\Big(\dot{u}\frac{\partial\delta\dot{w}_s}{\partial x} + \dot{u}\delta\frac{\partial\dot{w}_s}{\partial x} + \dot{v}\frac{\partial\delta\dot{w}_s}{\partial y} + \delta\dot{v}\frac{\partial\dot{w}_s}{\partial y} + I_2\left(\frac{\partial\dot{w}_b}{\partial x}\frac{\partial\delta\dot{w}_b}{\partial x} + \frac{\partial\delta\dot{w}_b}{\partial y}\frac{\partial\dot{w}_b}{\partial y}\right) + K_2\left(\frac{\partial\dot{w}_s}{\partial x}\frac{\partial\delta\dot{w}_s}{\partial x} + \frac{\partial\delta\dot{w}_s}{\partial y}\frac{\partial\dot{w}_s}{\partial y}\right) + J_2\left(\frac{\partial\dot{w}_b}{\partial x}\frac{\partial\delta\dot{w}_s}{\partial x} + \frac{\partial\delta\dot{w}_s}{\partial x}\frac{\partial\dot{w}_b}{\partial x} + \frac{\partial\dot{w}_b}{\partial y}\frac{\partial\delta\dot{w}_s}{\partial y} + \frac{\partial\delta\dot{w}_s}{\partial y}\frac{\partial\dot{w}_b}{\partial y}\right)\Big)\Big\} dA, \tag{14}$$

where dot-superscript convention indicates the differentiation with respect to the time variable t; $\rho(z)$ is the mass density; and (I_0, I_1, I_2, J_1, J_2, K_2) are mass inertias defined as

$$(I_0, I_1, I_2, J_1, J_2, K_2) = \int_{-\frac{h}{2}}^{\frac{h}{2}} (1, z, f, zf, z^2, f^2)\rho(z)dz \tag{15}$$

Substituting the expressions for δU, δV, δW, and δK from Eqs. (11)-(14) into Eq. (10), integrating by parts, collecting the coefficients of δu, δv, δw_b, δw_s, the following equations of motion of the nano-plate are obtained

$$\delta u: \frac{\partial N_x}{\partial x} + \frac{\partial N_{xy}}{\partial y} = (1 - (e_0 a)^2\nabla^2)\left(I_0\ddot{u} - I_1\frac{\partial\ddot{w}_b}{\partial x} - J_1\frac{\partial\ddot{w}_s}{\partial x}\right) \tag{16a}$$

$$\delta v: \frac{\partial N_{xy}}{\partial x} + \frac{\partial N_y}{\partial y} = (1 - (e_0 a)^2\nabla^2)\left(I_0\ddot{v} - I_1\frac{\partial\ddot{w}_b}{\partial y} - J_1\frac{\partial\ddot{w}_s}{\partial y}\right) \tag{16b}$$

$$\delta w_s: \frac{\partial^2 M_x^s}{\partial x^2} + 2\frac{\partial^2 M_{xy}^s}{\partial x\partial y} + \frac{\partial^2 M_y^s}{\partial y^2} + \frac{\partial Q_{xz}}{\partial x} + \frac{\partial Q_{yz}}{\partial y} = (1 - (e_0 a)^2\nabla^2)\Big(-F_{elastic} - q - N_x^0\frac{\partial^2(w_b + w_s)}{\partial x^2} - N_y^0\frac{\partial^2(w_b + w_s)}{\partial y^2} + I_o(\ddot{w_b} + \ddot{w_s}) + J_1\left(\frac{\partial\ddot{u}}{\partial x} + \frac{\partial\ddot{v}}{\partial y}\right) - J_2\nabla^2\ddot{w}_b - K_2\nabla^2\ddot{w}_s\Big) \tag{16c}$$

$$\delta w_b: \frac{\partial^2 M_x^b}{\partial x^2} + 2\frac{\partial^2 M_{xy}^b}{\partial x\partial y} + \frac{\partial^2 M_y^b}{\partial y^2} = (1 - (e_0 a)^2\nabla^2)\Big(-F_{elastic} - q - N_x^0\frac{\partial^2(w_b + w_s)}{\partial x^2} - N_y^0\frac{\partial^2(w_b + w_s)}{\partial y^2} + I_o(\ddot{w_b} + \ddot{w_s}) + I_1\left(\frac{\partial\ddot{u}}{\partial x} + \frac{\partial\ddot{v}}{\partial y}\right) - I_2\nabla^2\ddot{w}_b - J_2\nabla^2\ddot{w}_s\Big) \tag{16d}$$

By substituting Eq. (6) into Eq. (9) and the subsequent results into Eq. (12), the stress resultants are obtained as

$$\begin{Bmatrix} \{N\} \\ \{M^b\} \\ \{M^s\} \end{Bmatrix} = \begin{bmatrix} [A] & [B] & [B^s] \\ [B] & [D] & [D^s] \\ [B^s] & [D^s] & [H^s] \end{bmatrix} \begin{Bmatrix} \{\varepsilon^0\} \\ \{k^b\} \\ \{k^s\} \end{Bmatrix} and\ \{Q\} = [A^s]\{\gamma^s\} \tag{17}$$

where

$$([A],[B],[D],[B^s],[D^s],[H^s]) = \begin{bmatrix} 1 & v & 0 \\ v & 1 & 0 \\ 0 & 0 & \frac{1-v}{2} \end{bmatrix} (A, B, B^s, D, D^s, H^s) \tag{18}$$

$$(A, B, B^s, D, D^s, H^s) = \int_{-\frac{h}{2}}^{\frac{h}{2}} (1, z, f, z^2, zf, f^2) \frac{E(z)}{1-v^2} dz \tag{19}$$

$$[A^s] = \begin{bmatrix} 1 & 0 \\ 0 & 1 \end{bmatrix} A^s \ ,\ A^s = \int_{-h/2}^{h/2} \frac{E(z)}{2(1+v)} g^2 dz. \tag{20}$$

By substituting Eq. (17) into Eq. (16), the equations of motion can be expressed in terms of displacements (u, v, w_b, w_s) as

$$A\left(\frac{\partial^2 u}{\partial y^2} + \frac{1-v}{2}\frac{\partial^2 v}{\partial x^2} + \frac{1+v}{2}\frac{\partial^2 v}{\partial x \partial y}\right) - B\nabla^2 \frac{\partial w_b}{\partial x} - B^s \nabla^2 \frac{\partial w_s}{\partial x} = (1 - (e_0 a)^2 \nabla^2)\left(I_0 \ddot{u} - I_1 \frac{\partial \ddot{w}_b}{\partial x} - J_1 \frac{\partial \ddot{w}_s}{\partial x}\right) \tag{21}$$

$$A\left(\frac{\partial^2 v}{\partial y^2} + \frac{1-v}{2}\frac{\partial^2 v}{\partial x^2} + \frac{1+v}{2}\frac{\partial^2 u}{\partial x \partial y}\right) - B\nabla^2 \frac{\partial w_b}{\partial y} - B^s \nabla^2 \frac{\partial w_s}{\partial y} = (1 - (e_0 a)^2 \nabla^2)\left(I_0 \ddot{v} - I_1 \frac{\partial \ddot{w}_b}{\partial y} - J_1 \frac{\partial \ddot{w}_s}{\partial y}\right) \tag{22}$$

$$B\nabla^2\left(\frac{\partial u}{\partial x} + \frac{\partial v}{\partial y}\right) - D\nabla^4 w_b - D^s \nabla^4 w_b = (1 - (e_0 a)^2 \nabla^2)\Big(-F_{elastic} - q - N_x^0 \frac{\partial^2 (w_b + w_s)}{\partial x^2} - N_y^0 \frac{\partial^2 (w_b + w_s)}{\partial y^2} + I_0(\ddot{w}_b + \ddot{w}_s) + I_1\left(\frac{\partial \ddot{u}}{\partial x} + \frac{\partial \ddot{v}}{\partial y}\right) - I_2 \nabla^2 \ddot{w}_b - J_2 \nabla^2 \ddot{w}_s\Big) \tag{23}$$

$$B^s\nabla^2\left(\frac{\partial u}{\partial x} + \frac{\partial v}{\partial y}\right) - D^s\nabla^4 w_b - H^s \nabla^4 w_s - A^s \nabla^4 w_s = (1 - (e_0 a)^2 \nabla^2)\Big(-F_{elastic} - q - N_x^0 \frac{\partial^2 (w_b + w_s)}{\partial x^2} - N_y^0 \frac{\partial^2 (w_b + w_s)}{\partial y^2} + I_0(\ddot{w}_b + \ddot{w}_s) + J_1\left(\frac{\partial \ddot{u}}{\partial x} + \frac{\partial \ddot{v}}{\partial y}\right) - J_2 \nabla^2 \ddot{w}_b - K_2 \nabla^2 \ddot{w}_s\Big) \tag{24}$$

Clearly, when the effect of transverse shear deformation is neglected w_s=0, Eqs. (21)-(24) yields the equations of motion of FG nano-plate based on the classical plate theory.

3. Closed-form solution for bending analysis

In this section, a closed form solution for bending analysis of a FGM nano-plate is presented. For this purpose, the terms of kinetic energy in motion equations (i.e., Eqs. (21)-(24)) is neglected and it is assumed that the in-plane forces (i.e., N_x^0, N_y^0) are zero. Based on the Navier approach, the following expansions of displacements are chosen to automatically satisfy the simply supported boundary conditions of nano-plate

$$u(x,y,t)=\sum_{m=1}^{\infty}\sum_{n=1}^{\infty}U_{mn}\cos\alpha x\sin\beta y$$
$$v(x,y,t)=\sum_{m=1}^{\infty}\sum_{n=1}^{\infty}V_{mn}\sin\alpha x\cos\beta y$$
$$w_b(x,y,t)=\sum_{m=1}^{\infty}\sum_{n=1}^{\infty}W_{bmn}\sin\alpha x\sin\beta y$$
$$w_s(x,y,t)=\sum_{m=1}^{\infty}\sum_{n=1}^{\infty}W_{smn}\sin\alpha x\sin\beta y \tag{25}$$

where $=\sqrt{-1}$,$\alpha=\frac{m\pi}{a}$,$\beta=\frac{n\pi}{b}$,$U_{mn}, V_{mn}, W_{bmn}, W_{smn}$ are coefficients. The transverse load q is also expanded in the double-Fourier sine series as

$$q(x,y)=\sum_{m=1}^{\infty}\sum_{n=1}^{\infty}Q_{mn}\, sin\alpha x\sin\beta y \tag{26}$$

where

$$Q_{mn}=\frac{4}{ab}\int_0^a\int_0^b q(x,y)\, sin\alpha x\, sin\beta y\, dxdy=\begin{Bmatrix} q_0\ for\ \text{sinusoidally distributed load} \\ \frac{16q_0}{mn\pi^2}\ \text{for uniformly distributed load}\end{Bmatrix} \tag{27}$$

Substituting Eq. (25) into Eqs. (21)-(24), the closed-form solutions can be obtained from

$$\left(\begin{bmatrix} s_{11} & s_{12} & s_{13} & s_{14} \\ s_{12} & s_{22} & s_{23} & s_{24} \\ s_{13} & s_{23} & s_{33} & s_{34} \\ s_{14} & s_{24} & s_{34} & s_{44}\end{bmatrix}\right)\begin{Bmatrix} U_{mn} \\ V_{mn} \\ W_{bmn} \\ W_{smn}\end{Bmatrix}=\begin{Bmatrix} 0 \\ 0 \\ Q_{mn} \\ Q_{mn}\end{Bmatrix} \tag{28}$$

where

$$s_{11}=A\alpha^2+\frac{1-v}{2}A\beta^2,\qquad s_{12}=\frac{1+v}{2}A\alpha\beta,\qquad s_{22}=A\alpha^2\frac{1-v}{2}+A\beta^2$$
$$s_{13}=-B\alpha(\alpha^2+\beta^2),\qquad s_{14}=-B^s\alpha(\alpha^2+\beta^2),\qquad s_{23}=-B\beta(\alpha^2+\beta^2)$$
$$s_{24}=-B^s\beta(\alpha^2+\beta^2),$$
$$s_{33}=D(\alpha^2+\beta^2)^2+\left(1(e_0a)^2(\alpha^2+\beta^2)\right)\begin{pmatrix}-\mathrm{k}+G_\xi\left(-\cos^2\theta\alpha^2+2\alpha\beta\cos\theta\sin\theta-\sin^2\theta\beta^2\right) \\ +G_\eta\left(-\sin^2\theta\alpha^2-2\alpha\beta\sin\theta\cos\theta-\cos^2\theta\beta^2\right)\end{pmatrix},$$
$$s_{34}=D^s(\alpha^2+\beta^2)^2+\left(1(e_0a)^2(\alpha^2+\beta^2)\right)\begin{pmatrix}-\mathrm{k}+G_\xi\left(-\cos^2\theta\alpha^2+2\alpha\beta\cos\theta\sin\theta-\sin^2\theta\beta^2\right) \\ +G_\eta\left(-\sin^2\theta\alpha^2-2\alpha\beta\sin\theta\cos\theta-\cos^2\theta\beta^2\right)\end{pmatrix}$$
$$s_{44}=H^s(\alpha^2+\beta^2)^2+A^s(\alpha^2+\beta^2)^2 \tag{29}$$

4. Results and discussion

In this section, various numerical examples are presented and discussed to verify the accuracy of present theory in predicting the bending responses of simply supported FG nano-plates. For numerical results, an AL/AL_2o_3 nano-plate composed of aluminum (as metal) and alumina (as ceramic) is considered. The Young's modulus and density of aluminum are E_m=70 Gpa and

ρ_m=2702 kg/m^3 respectively, and those of alumina are E_c=380 Gpa and ρ_c=3800 kg/m^3 respectively. For verification purpose, the obtained results are compared with those predicted using various nano-plate theories. The Poisson's ratio of the nano-plate is assumed to be constant through the thickness and equal to 0.3. For convenience, the following non-dimensionalizations are used in presenting the numerical results in graphical and tabular form

$$\bar{w} = \frac{10E_c h^3}{q_0 a^4} w\left(\frac{a}{2},\frac{b}{2}\right),\ \bar{\sigma}_x = \frac{h}{q_0 a}\sigma_x\left(\frac{a}{b},\frac{b}{2},\frac{h}{2}\right),\ \bar{\sigma}_y = \frac{h}{q_0 a}\sigma_y\left(\frac{a}{b},\frac{b}{2},\frac{h}{3}\right),\ D = \frac{Eh^3}{12(1-v^2)}$$
$$\bar{\sigma}_{xy} = \frac{h}{q_0 a}\sigma_{xy}\left(0,0,\frac{h}{3}\right) \tag{30}$$

The first example is carried out for square plate subjected to uniformly distributed load (a=10 h) neglecting nonlocal parameter. Table 1 shows the comparison of non-dimensional deflections and stresses obtained by present theory with those given by Zenkour (2005) based on sinusoidal shear deformation theory (SSDT). It can be seen that the proposed new SSDT and conventional SSDT give identical results of deflections as well as stresses for all values of power law index p. It should be noted that the proposed new SSDT involves four unknowns as against five in case of conventional SSDT. It is observed that the stresses for a fully ceramic plate are the same as those for a fully metal plate. This is due to the fact that the plate for these two cases fully homogenous and the non-dimensional stresses do not depend on the value of the elastic modulus.

Table 1 Comparison of non-dimensional deflection and stresses of square plate under uniformly distributed load (a=10 h)

p	Method	$\bar{w}$	$\bar{\sigma}_x$	$\bar{\sigma}_y$	$\bar{\sigma}_{xy}$	$\bar{\sigma}_{yz}$	$\bar{\sigma}_{xz}$
Ceramic	Zenkour (2005)	0.4665	2.8932	1.9103	1.2850	0.4429	0.5114
	Present work	0.4665	2.8932	1.9103	1.2850	0.4429	0.5114
1	Zenkour (2005)	0.9287	4.4745	2.1962	1.1143	0.5446	0.5114
	Present work	0.9287	4.4745	2.1692	1.1143	0.5446	0.5114
2	Zenkour (2005)	1.1940	5.2296	2.0338	0.9907	0.5734	0.4700
	Present work	1.1940	5.2296	2.0338	0.9907	0.5734	0.4700
3	Zenkour (2005)	1.3200	5.6108	1.8593	1.0047	0.5629	0.4367
	Present work	1.3200	5.6108	1.8593	1.0047	0.5629	0.4367
4	Zenkour (2005)	1.3890	5.8915	1.7197	1.0298	0.5346	0.4204
	Present work	1.3890	5.8915	1.7197	1.0298	0.5346	0.4204
5	Zenkour (2005)	1.4356	6.1504	1.6104	1.0451	0.5031	0.4177
	Present work	1.4356	6.1504	1.6104	1.0451	0.5031	0.4177
6	Zenkour (2005)	1.4727	6.4043	1.5214	1.0536	0.4755	0.4227
	Present work	1.4727	6.4043	1.5214	1.0536	0.4755	0.4227
7	Zenkour (2005)	1.5049	6.6547	1.4467	1.0589	0.4543	0.4310
	Present work	1.5049	6.6547	1.4467	1.0589	0.4543	0.4310
8	Zenkour (2005)	1.5343	6.8999	1.3829	1.0628	0.4392	0.4399
	Present work	1.5343	6.8999	1.3829	1.0628	0.4392	0.4399
9	Zenkour (2005)	1.5876	7.1383	1.3283	1.0620	0.4291	0.4481
	Present work	1.5876	7.1383	1.3283	1.0620	0.4291	0.4481
10	Zenkour (2005)	1.5876	7.3689	1.2820	1.0694	0.4227	0.4552
	Present work	1.5876	7.3689	1.2820	1.0694	0.4227	0.4552
Metal	Zenkour (2005)	2.5327	2.8932	1.9103	1.2850	0.4429	0.5114
	Present work	2.5327	2.8932	1.9103	1.2580	0.4429	0.5114

Table 2 Comparison of non-dimensional deflection and stresses of square plate under sinusoidally distributed load (a=10 h)

p	Method	$\bar{w}$	$\bar{\sigma}_x$	$\bar{\sigma}_y$	$\bar{\sigma}_{xy}$	$\bar{\sigma}_{yz}$	$\bar{\sigma}_{xz}$
Ceramic	Benyoucef *et al*. (2010)	0.2960	1.9955	1.3121	0.7065	0.2132	0.2462
	Present work	0.2960	1.9955	1.3121	0.7065	0.2132	0.2462
1	Benyoucef *et al*. (2010)	0.5889	3.0870	1.4894	0.6110	0.2622	0.2462
	Present work	0.5889	3.0870	1.4894	0.6110	0.2622	0.2462
2	Benyoucef *et al*. (2010)	0.7572	3.6094	1.3954	0.5441	0.2763	0.2265
	Present work	0.7573	3.6094	1.3954	0.5441	0.2763	0.2265
3	Benyoucef *et al*. (2010)	0.8372	3.8742	1.2748	0.5525	0.2715	0.2107
	Present work	0.8377	3.8742	1.2748	0.5525	0.2715	0.2107
4	Benyoucef *et al*. (2010)	0.8810	4.0693	1.1783	0.5667	0.2580	0.2029
	Present work	0.8819	4.0693	1.1783	0.5667	0.2580	0.2029
5	Benyoucef *et al*. (2010)	0.9108	4.2488	1.1029	0.5755	0.2429	0.2017
	Present work	0.9118	4.2488	1.1029	0.5755	0.2429	0.2017
6	Benyoucef *et al*. (2010)	0.9345	4.4244	1.0417	0.5803	0.2296	0.2041
	Present work	0.9356	4.4244	1.0417	0.5803	0.2296	0.2041
7	Benyoucef *et al*. (2010)	0.9552	4.5971	0.9903	0.5834	0.2194	0.2081
	Present work	0.9562	4.5971	0.9903	035834	0.2194	0.2081
8	Benyoucef *et al*. (2010)	0.9741	4.7661	0.9466	0.5856	0.2121	0.2124
	Present work	0.9750	4.7661	0.9466	0.5856	0.2121	0.2124
9	Benyoucef *et al*. (2010)	0.9971	4.9303	0.9092	0.5875	0.2072	0.2164
	Present work	0.9925	4.9303	0.9092	0.5875	0.2072	0.2164
10	Benyoucef *et al*. (2010)	1.0083	5.0890	0.8775	0.5894	0.2041	0.2198
	Present work	1.0089	5.0890	0.8775	0.5894	0.2041	0.2198
Metal	Benyoucef *et al*. (2010)	1.6071	1.9955	1.3121	0.7065	0.2132	0.2462
	Present work	1.6070	1.9955	1.3121	0.7065	0.2132	0.2462

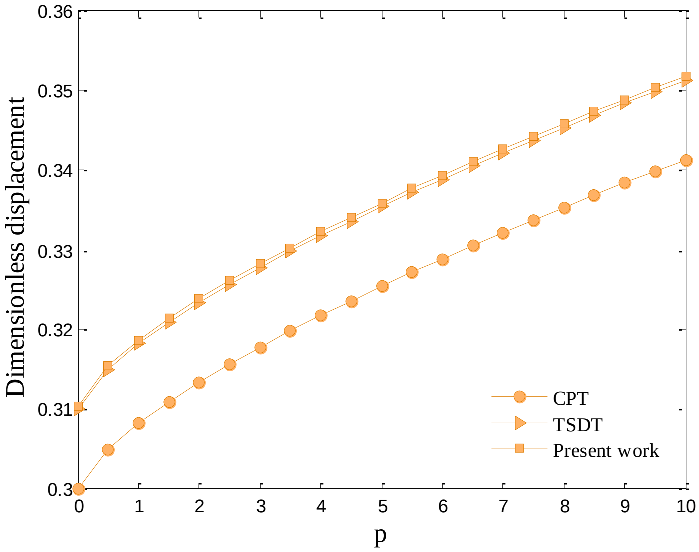

Fig. 1 Comparison of the variation of non-dimensional deflection of square nano-plate under sinusoidally distributed load versus power law index p (a=5 h)

Table 2 shows the comparison of non-dimensional deflections and stresses of square plate subjected to sinusoidally distributed load (a=10 h) neglecting nonlocal parameter. The obtained results are compared with those given by Benyoucef *et al*. (2010) based on the hyperbolic shear deformation theory (HSDT). It can be seen that an excellent agreement is obtained for all values of power law index p.

To illustrate the accuracy of present theory for wide range of power law index p, the variations of non-dimensional deflection $\bar{w}$ with respect to power law index p are illustrated in Fig. 1, for square nano-plate subjected to sinusoidally distributed load. The obtained results are compared with those predicted by CPT and TSDT (2000). It can be seen that the results of present theory and TSDT are almost identical, and the CPT underestimates the deflection of nano-plate.

The effect of the nano-plate length on the maximum deflection of the FG nano-plate with respect to power law index is shown in Fig. 2. It can be found that power law index can increase the deflection of the FG nano-plate. It is also observed that increasing the nano-plate length increases the deflection of the system. This is due to the fact that the increase of nano-plate length leads to a softer structure.

The effect of the elastic medium on the maximum deflection of the FG nano-plate with respect to power law index is illustrated in Fig. 3. In this figure four cases are considered which are without elastic medium, Winkler medium, Orthotropic Pasternak medium and Pasternak medium. As can be seen, considering elastic medium decreases maximum deflection of the FG nano-plate. It is due to the fact that considering elastic medium leads to stiffer structure. Furthermore, the effect of the Pasternak-type is higher than the Winkler-type on the maximum deflection of the FG nano-plate. It is perhaps due to the fact that the Winkler-type is capable to describe just normal load of the elastic medium while the Pasternak-type describes both transverse shear and normal loads of the elastic medium.

The effect of the orientation of foundation orthtotropy direction on the dimensionless displacement of the FG nano-plate versus power low index is depicted in Fig. 4. As can be seen,

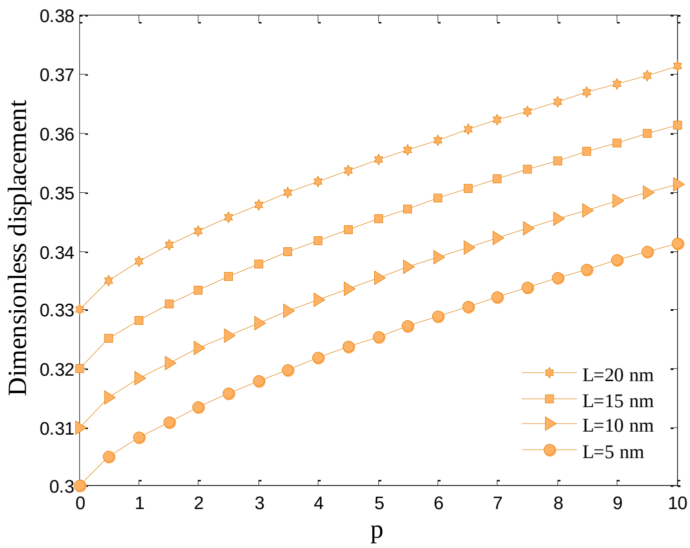

Fig. 2 The effect of the nano-plate length on the maximum deflection of system

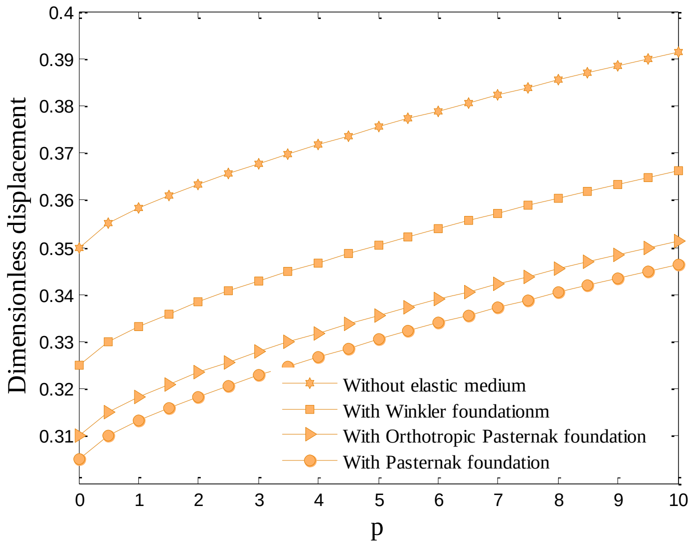

Fig. 3 The effect of the elastic medium on the maximum deflection of the FG nano-plate

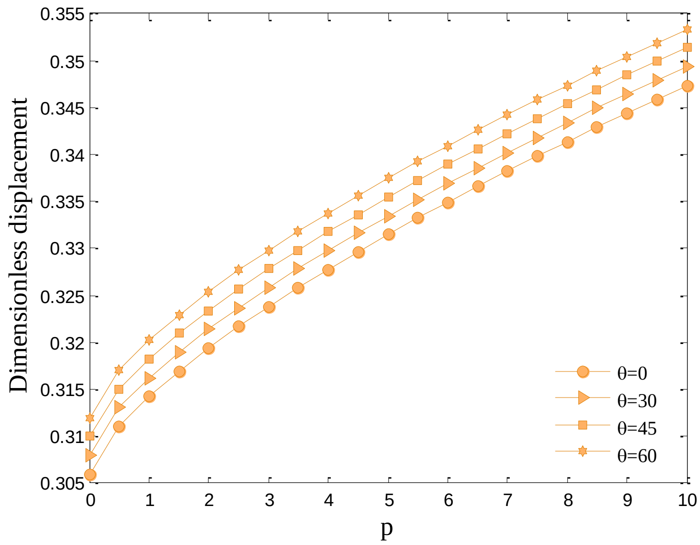

Fig. 4 The effect of the orientation of foundation orthtotropy direction on the maximum deflection of the FG nano-plate

with increasing orientation of foundation orthtotropy direction, the stiffness of structure decreases and consequently the dimensionless displacement of the FG nano-plate increases.

In order to show the effect of nonlocal parameter, Fig. 5 is plotted where the dimensionless displacement changes with power law index. As can be seen increasing the nonlocal parameter increases the dimensionless displacement. This is due to the fact that the increase of nonlocal parameter decreases the interaction force between nano-plate atoms, and that leads to a softer structure.

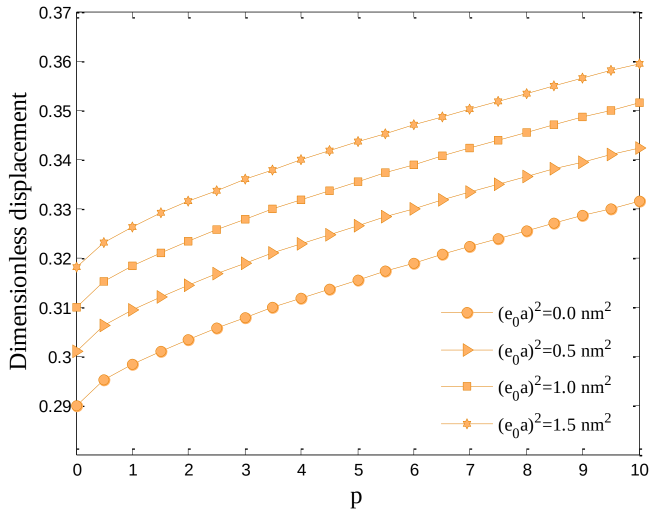

Fig. 5 The effect of the nonlocal parameter on the maximum deflection of the FG nano-plate

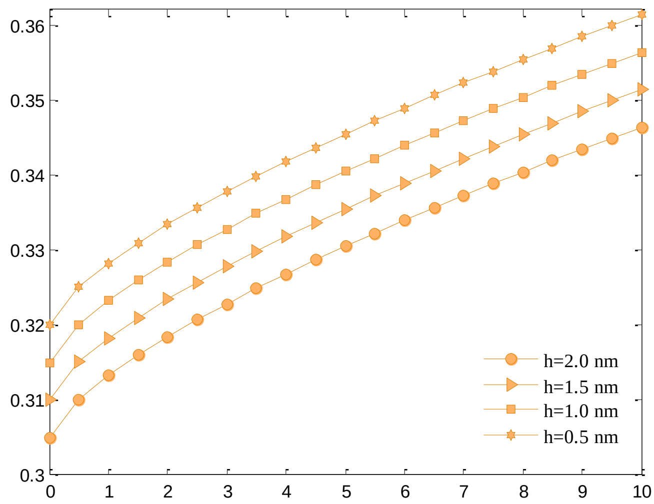

Fig. 6 The effect of the nano-plate thickness on the maximum deflection of the FG nano-plate

Fig. 6 illustrates the effect of nano-plate thickness on the dimensionless displacement of system versus power low index. It can be found that with increasing nano-plate thickness, the dimensionless displacement of structure decreases. This is because with increasing nano-plate thickness, the stiffness of system increases.

5. Conclusions

A new sinusoidal shear deformation theory is developed for bending of FG nano-plates. The small scale effects are considered based on Eringen's nonlocal theory. Equations of motion are derived from the Hamilton's principle. Closed-form solutions are obtained for simply supported nano-plates. All comparison studies show that the deflection and stress obtained by the proposed theory with four unknowns are almost identical with those predicted by other shear deformation theories containing five unknowns. The effects of different parameters such as nano-plate length and thickness, elastic foundation, orientation of foundation orthtotropy direction and nonlocal parameters are shown in dimensionless displacement of system. It can be found that increasing the nonlocal parameter increases the dimensionless displacement. It is also concluded that the effect of the Pasternak-type is higher than the Winkler-type on the maximum deflection of the FG nano-plate. Furthermore, considering elastic medium, decreases maximum deflection of the FG nano-plate. In addition, with increasing orientation of foundation orthtotropy direction, the stiffness of structure decreases and consequently the dimensionless displacement of the FG nano-plate increases.

References

Ameur, M., Tounsi, A., Mechab, I. and El Bedia, A.A., (2011), "A new trigonometric shear deformation theory for bending analysis of functionally graded plates resting on elastic foundations", *KSCE J. Civil Eng*., **15**, 1405-1414.

Benyoucef, S., Mechab, I., Tounsi, A., Fekrar, A., Ait Atmane, H. and Adda Bedia, E.A., (2010), "Bending of thick functionally graded plates resting on Winkler-Pasternak elastic foundations", *Mech. Compos. Mater*., **46**, 425-434.

Della Croce, L. and Venini, P. (2004), "Finite elements for functionally graded Reissner-Mindlin plates", *Comput. Meth. Appl. Mech. Eng*., **193**, 705-725.

Eringen, A.C. (1972), "Nonlocal polar elastic continua", *Int. J. Eng. Sci*., **10**, 1-16.

Fares, M.E., Elmarghany, M.K. and Atta, D. (2009), "An efficient and simple refined theory for bending and vibration of functionally graded plates", *Compos. Struct*., **91**, 296-305.

Javaheri, R. and Eslami, M.R. (2002), "Buckling of functionally graded plates under in-plane compressive loading", *J. Appl. Math. Mech*., **82**, 277-283.

Karama, M., Afaq, K.S. and Mistou, S. (2003), "Mechanical behaviour of laminated composite beam by the new multi-layered laminated composite structures model with transverse shear stress continuity", *Int. J. Solids Struct*., **40**, 1525-1546.

Matsunaga, H. (2008), "Free vibration and stability of functionally graded plates according to a 2-D higher-order deformation theory", *Compos. Struct*., **82**, 499-512.

Merdaci, S., Tounsi, A., Houari, M., Mechab, I., Hebali, H. and Benyoucef, S. (2011), "Two new refined shear displacement models for functionally graded sandwich plates", *Arch. Appl. Mech*., **81**, 1507-1522.

Pradyumna, S. and Bandyopadhyay, J.N. (2008), "Free vibration analysis of functionally graded curved panels using a higher-order finite element formulation", *J. Sound Vib*. **318**, 176-192.

Reddy J.N. (2000), "Analysis of functionally graded plates", *Int. J. Numer. Meth. Eng*., **47**, 663-684.

Talha, M. and Singh, B.N. (2010), "Static response and free vibration analysis of FGM plates using higher order shear deformation theory", *Appl. Math. Model*., **34**, 3991-4011.

Tounsi, A., Houari, M.S.A., Benyoucef, S. and Adda Bedia, E.A. (2011), "A refined trigonometric shear deformation theory for thermoelastic bending of functionally graded sandwich plates", *Aero. Sci. Tech.*, **24**, 563-572.

Xiao, J.R., Batra, R.C., Gilhooley, D.F., Gillespie, J.W. and McCarthy, M.A. (2007), "Analysis of thick plates by using a higher-order shear and normal deformable plate theory and MLPG method with radial basis functions", *Comput. Meth. Appl. Mech. Eng*., **196**, 979-987.

Zenkour, A.M. (2005), "A comprehensive analysis of functionally graded sandwich plates: Part 1-Deflection and stresses", *Int. J. Solid. Struct*., **42**, 5224-5242.

Xiang, S., Jin, Y.X., Bi, Z.Y., Jiang, S.X. and Yang, M.S. (2011), “A *n*-order shear deformation theory for free vibration of functionally graded and composite sandwich plates”, *Compos. Struct*., **93**, 2826-2832.

CC